Jordan Journal of Physics

ARTICLE

Second Virial Coefficient of Low-density Lithium-7 (^{7}Li) Gas in the Temperature Range 1 K–40000 K and Beyond

Mustafa M. Hawamdeh

Department of Physics, Faculty of Science, Al-Balqa Applied University, Al- Salt, Jordan.

Abstract: The second virial coefficient B for low-dense ^{7}Lithium (^{7}Li) gas is calculated over a wide temperature range 1 K–40000 K. In the 'high'-T limit (600 K–45000 K), the classical coefficient, B_{cl}, and the contribution of the first quantum-mechanical correction, B_{qc}, are computed from standard expressions, using a suitable binary potential. The classical coefficient, B_{cl}, together with the Boyle temperature, T_B, are determined and their values are in good agreement with previous results. In addition, the interface between the classical and quantum regimes is systematically investigated. Furthermore, the calculation of the quantum-mechanical second virial coefficient, B_q, is evaluated using the Beth-Uhlenbeck formula in the temperature range 1 K–500 K. A positive value of B_q indicates that the net interaction energy is repulsive, implying that the short-range repulsive forces dominate the long-range attractive forces. However, quite the opposite occurs for negative values of B_q, which are indicative of net attractive interaction. The general behavior of B_q is similar to the potential energy itself, such that the long-range attractive and the short-range repulsive potentials can be deduced from the measurements of B_q.

Keywords: Second virial coefficient, Low-density Lithium-7 Gas, Short-range repulsive forces, Long-range attractive forces.

PACS: 51.30.+i.

1. Introduction

This paper is a theoretical study of the second virial coefficient B over a wide temperature range (1 K–40000 K). In the high temperature limit (600 K–40000 K and beyond), B is most likely to behave classically. Therefore, we focus on the classical second virial coefficient (B_{cl}) and the contribution of the first quantum correction (B_{qc}). In the low temperature limit (1 K–100 K), we focus on the quantum second virial coefficient (B_q). To investigate the boundary line between the classical and quantum regimes, we focus on the intermediate temperature range from (100 K–500 K).

The temperature-dependent second virial coefficient B(T) is a basic thermodynamic parameter and is important for representing the equation of state of the system P-V-T (pressure–volume–temperature), describing the behavior of real, low-density gases. In general, it is characteristic of the interaction potential between the particles. It represents the non-ideality of gas behavior arising due to the two-body interactions between atoms. Also, the sign of the second virial coefficient reflects how much the contribution of the attractive and repulsive parts of the potentials [1-4]. The intermolecular potential can be developed from experimental measurements of B [5], as there are many methods like static light scattering (SLS) [6]. B acts as an indicator of the classical-quantum borderline in a nonideal gas [4]. Moreover, it provides the connection between the microscopic and macroscopic properties, such as how the binary interactions affect the thermodynamic properties of a physical system. Most interestingly, B_q can provide information about

---

the possibility of the formation of small clusters [7].

Quite a number of studies calculated the second virial coefficients of all the alkali vapors over a wide range of temperatures using different potentials. For example, Sannigrahi *et al.* [8] used the Morse and Rydberg potentials for the ground singlet state and their anti-Morse potential for the triplet state. Nieto de Castro *et al.* [9] used the two-body interaction potential energy functions for the ground singlet state and excited triplet states of the alkali atoms proposed by Varandas *et al.* [10]. Mies and Julienne [11] used an electronic-rotational potential and Moncef [12] used the Rydberg-Klein-Rees interatomic singlet and triplet potentials.

The main input in calculating B is the interaction potential. In this work, we have used the singlet $X\ ^1\Sigma+g$ and triplet $a\ ^3\Sigma+u$ interatomic potentials as constructed for different three potentials; namely, Morse, Rydberg and the modified Morse potentials. A brief description of them is presented in Section 2 which is specified for the theoretical framework. In Section 3, the results are presented and discussed thoroughly with suitable comparisons. In Section 4, the paper ends with a short conclusion.

2. Theoretical Formalism

2.1 Classical Virial Coefficient

The simple classical expressions of the second virial coefficient and its quantum correction as functions of temperature *T*, are given by [13, 14]:

$$B_{cl}(T) = 2\pi \int_0^\infty [1 - e^{-\beta V(r)}] r^2 dr; \qquad (1)$$

$$B_{qc}(T) = \frac{\pi \hbar^2 \beta^3}{6m} \int_0^\infty [e^{-\beta V(r)}] (V'(r))^2 r^2 dr \qquad (2)$$

where $\hbar, \beta, m$ denote the reduced Planck's constant, the inverse temperature parameter $(k_B T)^{-1}$, k_B Boltzmann's constant, and the mass of the ^{7}Li atom, respectively. T is the temperature in Kelvin, V(r) is the pair interatomic potential and V'(r) is its first derivative with respect to the argument r.

The total second virial coefficient for a gas of atoms which interact via singlet and triplet potentials was given by Sinanoglu and Pitzer [15] and reads:

$$B = \frac{1}{4} B_2^{(s)} + \frac{3}{4} B_2^{(t)}, \qquad (3)$$

$B_2^{(s)}$ and $B_2^{(t)}$ being the the virial coefficients obtained from the interaction potential energy function for the different singlet and triplet-spin energy states, respectively. The first two potentials used are the Morse $U_M{}^s(r)$ and Rydberg $U_R{}^s(r)$ potentials for singlet states, which are given by:

$$U_M{}^s(r) = U_e[e^{-2ax} - 2e^{-ax}] \qquad (4a)$$

$$U_R{}^s(r) = U_e[e^{-bx}](1 + bx) \qquad (4b)$$

where $a = r_e(\kappa_e/2U_e)^{1/2}$, $x = \frac{r}{r_e} - 1$, $b = \sqrt{2}a$ and κ_e is the vibrational force constant of the diatomic alkali metal molecules. Here, the U_e, r_e, k_e are constants and are listed in Table 1. The anti-Morse potential $U^t(r)$ was proposed by [8] for the triplet state and is given by:

$$U^t(r) = 0.4427\ U_e[e^{-2ax} + 0.092\ e^{-ax}]. \qquad (5)$$

The anti-Morse function is a repulsive potential and goes to zero at infinite distance. Eq. (5) expresses the triplet-state potential in terms of ground-state potential parameters.

TABLE 1. Parameters of the Morse and anti-Morse potentials.

Parameter	Value
U_e	1.06 eV
r_e	2.65
κ_e	0.254

The third potential used is the modified Morse potential (HH-potential) [16]. It depends on the two-body Li atom interactions and is taken in the present work as the HH-hybrid potential for the singlet and triplet states [16-18]. The HH-potential is given by [16]:

$$V^*(r^*) =$$
$$\varepsilon' \left\{ \begin{array}{c} \exp\left[-2a\left(\frac{r^*}{d} - 1\right);\right] \\ -2\exp\left[-a\left(\frac{r^*}{d} - 1\right)\right] \\ +\beta\left(\frac{r^*}{d} - 1\right)^3 \times \\ \left[1 + \gamma\left(\frac{r^*}{d} - 1\right)\right]\exp\left[-2a\left(\frac{r^*}{d} - 1\right)\right] \end{array} \right\}; \qquad (6)$$

where $V^* = \frac{v}{\varepsilon}$; $r^* = \frac{r}{\sigma}$; $d = \frac{r_e}{\sigma}$; $\sigma = 3.24$Å;

$a = \frac{\omega_e}{2\sqrt{\beta_e \varepsilon'}}$; $\beta = ca^3$; $\gamma = ba$; $c = 1 + a_1\sqrt{\frac{\varepsilon'}{a_o}}$;

$b = 2 - \frac{\frac{7}{12} - \varepsilon'\frac{a_2}{a_o}}{c}$; $a_0 = \frac{\omega_e{}^2}{4\beta_e}$; $a_1 = -1 - \frac{\alpha_e\omega_e}{6\beta_e^2}$;

$a_2 = \frac{5}{4}a_1^2 - \frac{2\omega_e\chi_e}{3\beta_e}$, ε' being the well depth in cm^{-1}.

This potential depends on the spectroscopic constants, the well depth ε', the fundamental vibration frequency ω_e, the anharmonicity constant $\omega_e \chi_e$, the rotational constant β_e, the vibration-rotation coupling constant α_e and the equilibrium internuclear separation r_e of the atoms in the dimer. The latter are listed for the singlet and triplet states of Li in Table 2 [16-18]. The Li-Li potentials for the singlet $x^1 \sum_g^+$ and triplet $x^3 \sum_u^+$ states are plotted as shown in Fig.1.

TABLE 2. HH parameters for the states $x^1 \sum_g^+$ and $a^3 \sum_u^+$ of Li, as obtained from the spectroscopic constants.

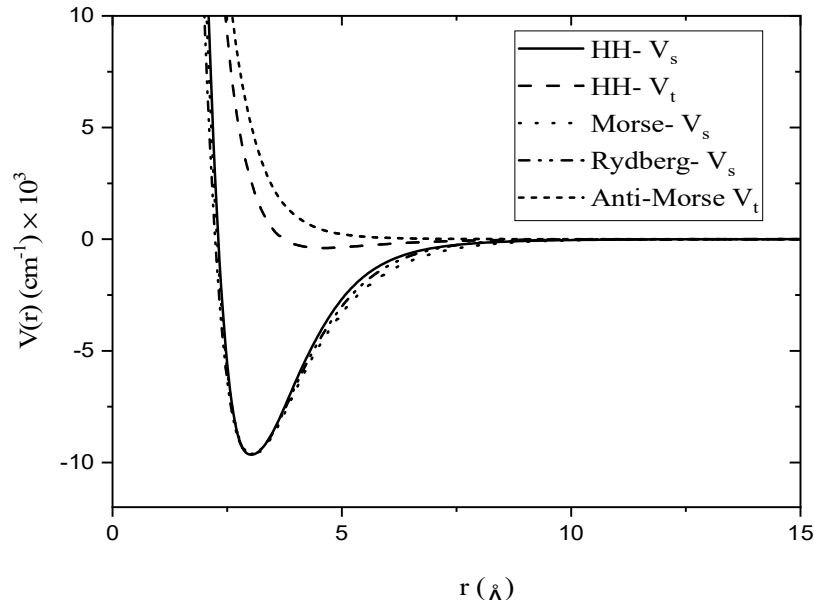| Parameter	$x^1 \sum_g^+$ [16]	$a^3 \sum_u^+$ [17, 18]
ε'	8614 (cm^{-1})	338.71(cm^{-1})
ω_e	351.43 (cm^{-1})	64.88 (cm^{-1})
$\omega_e \chi_e$	2.61 (cm^{-1})	3.41 (cm^{-1})
β_e	0.67264 (cm^{-1})	0.279 (cm^{-1})
α_e	0.00704 (cm^{-1})	0.0187 (cm^{-1})
r_e	2.6729 Å	4.154 Å

FIG. 1. Li-Li potentials for the singlet $x^1 \sum_g^+$ and triplet $x^3 \sum_u^+$ states, the HH-potential and Morse and Rydberg potentials.

2.2 Quantum Second Virial Coefficient, B_q

The Uhlenbeck and Beth formula for the quantum second virial coefficient at low temperatures is given by [19, 20]:

$$B_q(T) = -\frac{\lambda^3}{2^{5/2}} - 2^{3/2}\lambda^3 \sum_{E_B}\left(e^{-\beta E_B} - 1\right) - \frac{2^{3/2}\lambda^5}{\pi^2}\int_0^\infty dk\, k \sum_l{}'(2l+1)\delta_l(k)e^{-\beta E(k)} \quad (7)$$

Eq. (7) contains three terms: B_{ideal}, B_{bound} and B_{phase}. B_{ideal} is the quantum ideal-gas term. This is dominant in the low-temperature region; it goes to zero at large T. B_{bound} is the term consisting of the discrete energy spectrum made possible by the two-body interaction, where E_B are the bound-state energies. The latter is ignored for the Lithium system, since it is unbounded in the T-range of this study. Finally, B_{phase} denotes the contribution of the scattering-state continuum, where $\delta_\ell(k)$ stands for the scattering phase of the lth partial wave of wavenumber k that arises because of the pair interaction V(r). The factor $(2l+1)$ for the degenerate state comes from the magnetic quantum number m and the primed summation $\sum_l{}'$ goes over even ℓ values in the case of bosons. The bound state term (discrete-state contribution) can be neglected, because it is quite small. Therefore, the two contributions to the overall value of B_q are the quantum ideal-gas term and the scattering term (continuum-state contribution).

The phase-shifts $\delta_\ell(k)$ can be obtained numerically from the solution of the Lippmann-Schwinger (LS) integral equation which describes momentum space scattering in terms of

241

the T-matrix, using a matrix-inversion technique. The LS formalism is well-described elsewhere [21-23]. The basic input in computing is the interatomic potential.

Throughout our work, we used natural units such that $\hbar, m, k_B$ are exactly equal to 1 and applied the conversion factor $\dfrac{\hbar^2}{m} = 6.919 \text{ K.Å}^2$. In this system, all physical quantities can be expressed in terms of [length, L]. One can easily go back to SI units through the conversion factor quoted.

3. Results and Discussion

3.1 Classical Second Virial Coefficient with First Quantum Correction, B_{qc}

Our results for the classical second virial coefficient B_{cl} and the first quantum correction

B_{qc} are shown in Tables 3-7 and Fig. 2. Table 3 shows B_{cl}, B_{qc} and B_{total} in the T-range 600 K to 45000 K for the singlet (Morse and Rydberg potentials) and anti-Morse potential for the triplet state. B_{total} is calculated by adding B_{qc} to B_{cl}. It is found that B_{total} is negative, but it increases (i.e., its absolute value decreases) as T rises. The negative sign means that the interaction is attractive. At a certain $T \equiv T_B$ (*Boyle's temperature*), B_{total} = zero. This occurs when the attractive forces balance exactly the repulsive forces. In Table 4, the present results for the Boyle temperature T_B are compared to previous results [8] displaying good agreement. By increasing T (T >T_B), B_{total} becomes positive because of the repulsive forces. For the HH potential, B_{total} equals zero at T = 126852 K. It is very high compared to the previous calculated value from the Morse and Rydberg potentials.

TABLE 3. The classical second virial coefficient B_{cl} (cm^3/mole) and first quantum correction B_{qc} (cm^3/mole), at different temperatures T [K] for singlet (Morse and Rydberg potentials) and triplet state (using anti-Morse potential).

T[K]	Morse		Rydberg		Anti-Morse		B_{total} [cm^3/mole]	
	B^s_{cl} [cm^3/mole]	B^s_{qc} [cm^3/mole]	B^s_{cl} [m^3/mole]	B^s_{qc} [cm^3/mole]	B^t_{cl} [cm^3/mole]	B^t_{qc} [cm^3/mole]	Morse	Rydberg
600	-1.02×10^{10}	2.78×10^8	-1.02×10^{10}	2.78×10^8	134.7	0.0825	-2.50×10^9	-2.49×10^9
700	-6.02×10^8	1.18×10^7	-5.98×10^8	1.18×10^7	125.7	0.06768	-1.47×10^8	-1.47×10^8
800	-7.24×10^7	1.07×10^6	-7.20×10^7	1.07×10^6	118.4	0.05694	-1.78×10^7	-1.77×10^7
900	-1.41×10^7	1.6×10^5	-1.40×10^7	1.61×10^5	112.2	0.04885	-3.48×10^6	-3.46×10^6
1000	-3.84×10^6	3.50×10^5	-3.81×10^6	3.50×10^5	106.9	0.04255	-9.51×10^5	-9.43×10^5
1200	-5.58×10^5	3401	-5.52×10^5	3.40×10^3	98.19	0.03346	-1.39×10^5	-1.37×10^5
1400	-1.44×10^5	619.1	-1.42×10^5	618.43	91.31	0.02726	-3.58×10^4	-3.53×10^4
1600	-8.44×10^4	167.5	-5.23×10^4	167.30	85.68	0.02279	-2.10×10^3	-1.29×10^4
1800	-2.49×10^4	59.22	-2.43×10^4	59.12	80.95	0.01945	-6.14×10^3	-6.01×10^3
2000	-1.37×10^4	25.29	-1.34×10^4	25.24	76.9029	0.0168544	-3.37×10^3	-3.28×10^3
2400	-5.77×10^3	6.76	-5.57×10^3	6.744	70.29	0.013132	-1.39×10^3	-1.34×10^3
2800	-3.17×10^3	2.527	-3.03×10^3	2.516	65.06	0.01061	-743	-709
3000	-2.51×10^3	1.681	-2.39×10^3	1.673	62.82	0.009640	-579	-549
3500	-1.57×10^3	0.7223	-1.48×10^3	0.7177	58.04	0.007767	-349	-327
4000	-1.12×10^3	0.3706	-1.04×10^3	0.3675	54.14	0.006430	-237	-219
5000	-674.5	0.1359	-624.4	0.1343	48.08	0.004671	-133	-120
6000	-476.1	0.06533	-437.2	0.06427	43.54	0.003583	-86.4	-76.6
10000	-212.1	0.01149	-191.6	---	32.57	0.00167	-28.6	-23.5
15000	-123.1	0.003676	-110.2	---	25.50	0.000888	-11.7	-8.43
20000	-86.01	0.001789	-76.65	---	21.25	0.000558	-5.56	-3.22
25000	-65.76	0.001062	-58.44	---	18.35	0.000385	-2.68	-0.845
28000	-57.52	0.001022	-51.05	---	17.00	0.000324	-1.63	-0.00089
29000	-55.19	0.000932	-48.97	---	16.60	0.000301	-1.35	0.210
30000	-53.0	0.000707	-47.05	---	16.22	0.000282	-1.09	0.405
35000	-44.34	0.000506	-39.27	---	14.58	0.000215	-0.152	1.11
36000	-42.92	0.000476	-38.00	---	14.29	0.0002047	-0.0114	1.22
37000	-41.58	0.000449	-36.81	---	14.02	0.000195	0.117	1.31
40000	-38.01	0.00038	-33.63	---	13.26	0.000169	0.442	1.54
45000	-33.21	0.000297	-29.36	---	12.18	0.000137	0.831	1.79

TABLE 4. Boyle temperatures T_B [K] compared to previous results [8].

T_B [K]			
Present results		[8]	
Morse	Rydberg	Morse	Rydberg
36086	28039	31244	23799

Fig. 2 displays B_{total} in the T-range 500 K–30000 K. B_{total} continues to increase with increasing T, but it changes relatively slowly at the higher T values. It is expected that B_{total} flattens out while dropping slowly toward zero at significantly higher temperatures. It is noted that the second virial coefficient is positive or negative depending on the temperature. The explanation for this T-behavior of B_{cl} is as follows: the negative values of B are indicative of a net attractive interaction between the particles; conversely, a positive value is an indication that the net interaction energy is repulsive. If B equals zero, then no interactions are present and the virial equation reduces to the equation of state for the ideal gas. The figure shows that at low temperatures, B is largely negative, but above a certain temperature, it becomes positive and less dependent on temperature. At low T, the weak attractive part of the potential dominates the low kinetic energy of Li atoms, leading to a negative B_{cl}. As temperature increases, atoms become more energetic, increasing the contribution of short-range repulsive forces and causing B to become less negative. In contrast, at high T, the large kinetic energy of the Li atoms leads to a net repulsive interaction among them, yielding thereby a positive B. At high T, B increases slowly with temperature.
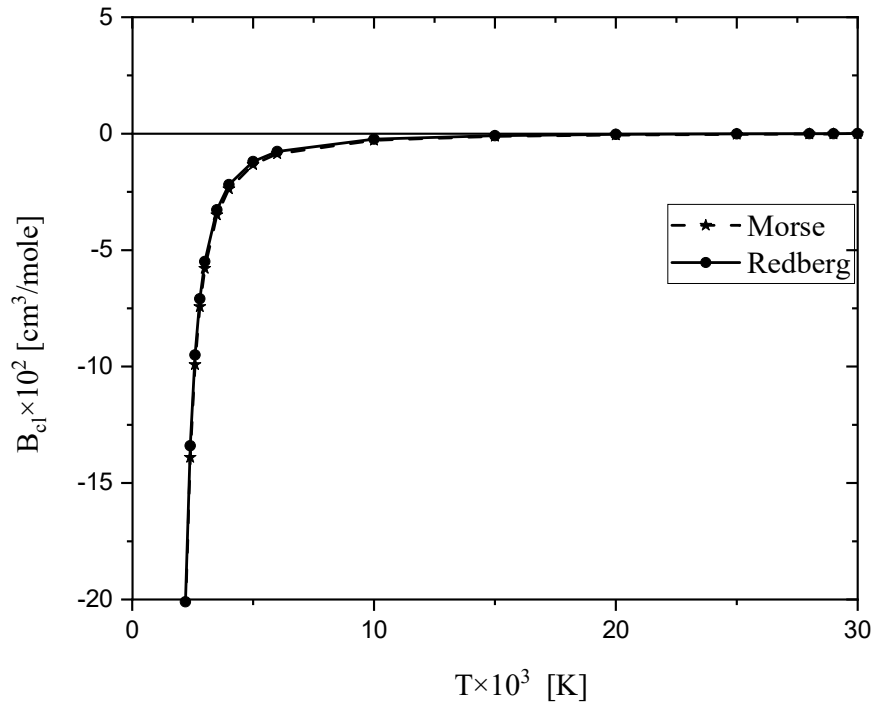

FIG. 2. The total classical second virial coefficient B_{cl} [cm^3/mole] as a function of temperature T [K] using Morse and Rydberg potentials.

In order to test the reliability of the present calculation, we have used a third potential; namely the modified Morse potential (HH-potential). In Tables 5 and 6, the present results for B_{total} are compared to previous results in [8, 9, 11, 16, 24]. It is noted that the present results are of the same order of magnitude as the previous results. The values of the first quantum correction B_{qc} from 600 K to 45000 K are positive and decrease to zero at T= 6000 K, as shown in Table 6. In Table 7, B_{cl}, B_{qc} (for singlet and triplet states) and B_{total} are calculated in the T-range (100 K–500 K). It is noted that B^s_{qc} plays a significant role in this T-range and the quantum effects cannot be ignored in this range. It is clear that it becomes greater than $\left| B_{cl} \right|$ at T $\leq$ 100 K, Therefore, the classical expression fails; so that B_q must be used instead.

TABLE 5. The total classical second virial coefficient B_{total} [cm^3/mole] at different temperatures T. Previous results [8] are included for comparison purposes.

| T [K] | B_{total} [cm^3/mol] | | | |
| | Present results | | [8] | |
	Morse	Rydberg	Morse	Rydberg
2460.253	-1244	-1201.9	-1225.3	-1201.5
4100.422	-220.8	-204.2	-218.6	-276.6
6150.632	-81.6	-72.3	-80.7	-203.4
8200.843	-43.6	-37.1	-42.9	-71.4
12301.26	-18.3	-14.3	-17.6	-36.2
16401.69	-9.4	-6.5	-8.9	-13.3
24602.53	-2.8	-0.98	-2.5	-5.2

TABLE 6. Comparison between the present results for B_{cl} and B_{qc} and previous results.

T[K]	B_{total} [m^3/mol] Present result	B_{total} [m^3/mol] [9]	B_{total} [m^3/mol] [11]	B_{total} [m^3/mol] [16]*	B_{total} [m^3/mol] [24]
500	-1.624 x 10^5	---	-1.073 x 10^5	-1.167 x 10^6	---
600	-2923	---	-2060	-6551	---
700	-167.9	---	-124.2	-575.1	---
800	-19.93	-14.93	-15.28	-69.83	---
900	-3.831	-2.963	-3.023	-10.85	-9.647
1000	-1.032	-0.8191	-0.8335	-2.059	-2.370
1200	-0.1472	-0.1213	-0.1229	-0.1155	-0.2941
1400	-0.0374	-0.03164	-0.03197	-0.03996	-0.06746
1600	-0.01361	-0.01174	-0.01184	-0.01681	-0.02265
1800	-0.00629	-0.005509	-0.005538	-0.007809	-0.00977
2000	-0.00344	-0.003039	-0.003048	-0.003962	-0.00502
2200	-0.00212	----	-0.001885	-0.002130	-0.00289
2400	-0.00143	----	-0.00127	-0.001219	-0.00182
2500	-0.0012	-0.001071	-0.001069	-0.001037	-0.00146
3000	-0.00061	-0.000544	-0.000541	-0.000557	----
3500	-0.00031	----	-0.000333	-0.000329	----
4000	-0.00026	----	-0.00023	-0.000228	----
4500	-0.00019	----	-0.000172	-0.000172	----
5000	-0.00017	----	-0.000135	-0.000133	----
5500	-0.00013	----	-0.00011	-0.000109	----
6000	-0.00011	----	-0.0000915	-0.000092	----

*The result of Holand *et al.* [16] is published in their work as a ratio from Mise and Julienne [11].

TABLE 7. B_{cl}, B_{qc} (for singlet and triplet states) and B_{total} in the T-range (100–500 K).

T[K]	B^s_{cl} [m^3/mol]	B^s_{qc} [m^3/mol]	B^t_{cl} [m^3/mol]	B^t_{qc} [m^3/mol]	B_{total} [m^3/mol]
100	-3.359×10^{54}	3.538×10^{54}	-11587.1	289.7	4.475×10^{52}
200	-5.582×10^{27}	1.526×10^{27}	-1520.5	8.315	-1.014×10^{27}
300	-7.739×10^{18}	8.857×10^{17}	-709.1	1.910	-1.713×10^{18}
400	-2.948×10^{14}	1.876×10^{13}	-447.2	0.8020	-6.901×10^{13}
500	-6.770×10^{11}	2.725×10^{10}	-320.7	0.4419	-1.624×10^{11}

3.2 Quantum Second Virial Coefficient, B_q

Our results for B_q are given in Table 8 and Fig. 3 for the T-range (1–500 K) in the zero-density limit. In this regime, the system is considered to be in the vapor phase. At very low T, B_q is positive indicating that the repulsive part of the potential is dominant. As T is increased, the attractive part becomes more dominant. The negativity of B_q rises with increasing T until it approaches a minimum at T_{min}. For $T > T_{min}$, B_q becomes less negative with increasing T, going to zero in the high limit of T. This behavior is an evidence of quantum effects. The overall behavior of B_q is the same as that of the potential itself. In the Morse and Rydberg potentials, B_q changes sign at T = 80 K and T= 90 K, respectively, from positive to negative, but for the HH-potential, B_q changes sign at T=7 K from positive to negative. This means the HH potential is more attractive than the two other

potentials, since the triplet part in the Morse and Rydberg potentials is completely repulsive.

The general behavior of B_q (Fig. 3) is the same as that of the Li-Li potential V(r) itself (Fig. 1). This behavior reflects that the short-range repulsive component and the long-range attractive component with the minimum in between represent equilibrium [1]. Moreover, it is concluded that the HH-potential is the most attractive potential. The behavior of B_q must be quantum-mechanical in origin. The classical calculation of B yields a large and negative value at low temperatures in the presence of an attractive well. This behavior occurs because of the uncertainty principle. At these low temperatures, the thermal de Broglie wavelength of Li is several tens of Ångstroms, which is probably enough to "wash out" the potential energy bottom, thereby resulting in an overall repulsive interaction.

TABLE 8. The quantum second virial coefficient B_q [m^3/mole] as a function of temperature T [K] using Morse, Rydberg and HH potentials.

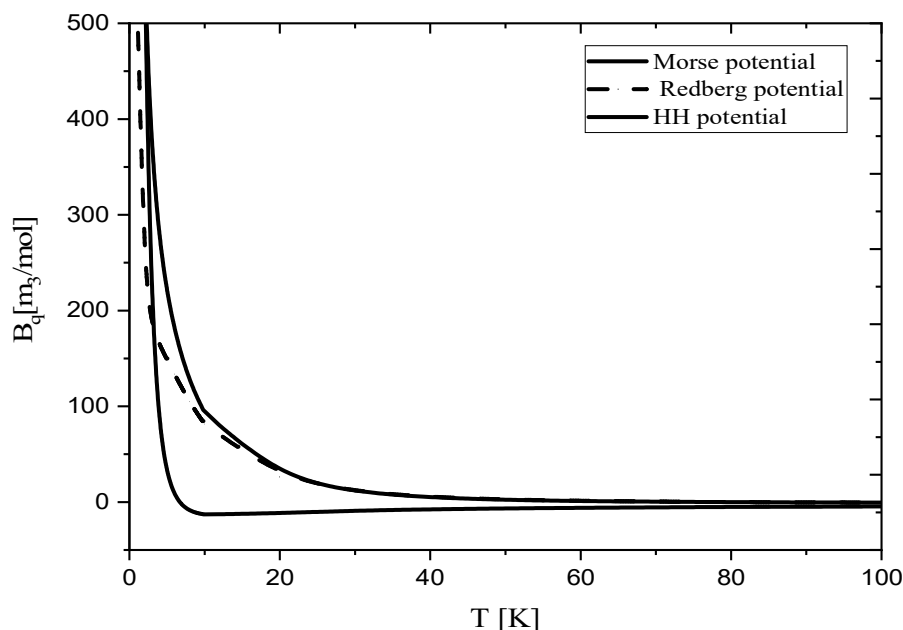|	B_q[m^3/mol]		
T [K]	Morse potential	Rydberg potential	HH potential
1	992.5	531.1	1418.4
2	531.2	235.4	495.3
4	274.8	164.6	78.53
6	180.7	133.6	7.331
7	151.1	118.8	-3.392
8	127.7	105.0	-8.781
10	93.40	81.52	-12.89
30	10.38	10.91	-8.948
50	2.251	2.679	-6.532
70	0.3642	0.5211	-5.463
90	-0.2945	-0.3277	-4.790
100	-0.4742	-0.5728	-4.520
200	-1.160	-1.399	-2.756
300	-1.347	-1.515	-1.777
400	-1.345	-1.458	-1.226
500	-1.267	-1.345	-0.9168

FIG. 3. The quantum second virial coefficient B_q [cm^3/mole] as a function of temperature T [K] using Morse, Rydberg and HH potentials.

4. Conclusion

This work has addressed the second virial coefficient B of low-density ^{7}Li vapor, using the Morse, Redberg and HH-potentials, in the temperature-range 1 K–45000 K and beyond. This range spans the quantum as well as classical regimes. Accordingly, the centerpiece of this work includes the calculation of the classical coefficient B_{cl} together with the first quantum correction B_{qc} and the quantum coefficient B_q. Also, the interface between the classical and quantum regimes is systematically investigated.

The main objectives of this work were to calculate the classical second virial coefficient B_{cl}, the first quantum correction B_{qc} to this coefficient in the T-range 100 K–40000 K and beyond and to determine the quantum counterpart B_q in the T-range 1 K–500 K. A positive value of B_q indicates that the net interaction energy is repulsive implying an overall repulsive effective interaction; whereas the negative values of B_q are indicative of a net attractive interaction.

It has been found that the general behavior of B_q is the same as that of the potential itself, such that the short-range repulsive and long-range attractive potentials could be deduced from the result of B_q. There seems to be an almost one-to-one correspondence between the respective repulsive, attractive and 'minimum' regions. Thus, information about diatomic interactions is contained in B.

In conclusion, the results show that B is a sharp indicator of the demarcation between the classical and quantum regimes. In the high-T limit, B is expected to behave classically; whereas it should behave quantum-mechanically at 'low' T. There are some problems that one can pursue starting with the present work. One problem is using the present formalism for exploring the gas of Lithium isotope (^{6}Li) which is a Fermi system. It would be interesting to observe the similarities and differences. Another problem is the calculation of the second virial coefficient for other atomic gases, such as Na and K.

References:

[1] Al-Obeidat, O.T., Sandouqa, A.S., Joudeh, B.R., Ghassib, H.B. and Hawamdeh, M.M., Can. J. Phys., 95 (12) (2017) 1208.

[2] Mosameh, S.M., Sandouqa, A.S., Ghassib, H.B. and Joudeh, B. R., J. Low Temp. Phys., 175 (2014) 523.

[3] Van Rijssel, J., Peters, V.F.D., Meeldijk, J.D., Kortschot, R.J., van Dijk-Moes, R.J.A., Petukhov, A.V., Erné, B.H. and Philips, A.P., J. Phys. Chem. B, 118 (2014) 11000.

[4] Ghassib, H.B., Sandouqa, A.S., Joudeh, B.R. and Mosameh, S.M., Can. J. Phys., 92 (9) (2014) 997.

[5] Laurendeau, N.M., "Statistical Thermodynamics: Fundamentals and Applications". (Cambridge University Press, 2005).

[6] Velev, O.D., Kaler, E.W. et al., Biophys. J., 75 (6) (1998) 2682.

[7] Sandouqa, A.S., Chem. Phys. Lett., 703 (2018) 29.

[8] Sannigrahi, A.B., Noor Mohammad, S. and Mookherjee, D.C., The Journal of Chemical Physics 63 (1975) 12; Sannigrahi, A.B. and Noor Mohammad, S., Molecular Physics, 31 (3) (1976) 963.

[9] Nieto de Castro, C.A., Fareleira, J.M.N.A., Matias, P.M., Ramires, M.L.V., Pais, A.A.C.C. and Varandas, A.J.C., Ber. Bunsenges. Phys. Chem., 94 (1990) 53.

[10] Varandas, A.J.C., J. Chem. SOC. Faraday Trans., 11 (76) (1980) 129; Varandas, A.J.C. and Brandgo, J., Mol. Phys., 45 (1982) 857.

[11] Mies, F.H. and Julienne, P.S., J. Chem. Phys., 77(12) (1982) 15 Dec.

[12] Moncef, B., J. Plasma Fusion Res. Series, 7 (2006) 217.

[13] Mello, E.V.L., Rehr, J.J. and Vilches, O.E., Phys. Rev. B, 28 (7) (1983) 3759.

[14] Pack, R.T., J. Chem. Phys., 78 (1983) 7217.

[15] Sinanoglu, O. and Pitzer, K.S., J. Chem. Phys., 31 (1960) 960.

[16] Holland, P.M., Biolsi, L. and Rainwater, J.C., J. Chem. Phys., 85 (1986) 4011.

[17] Halls, M.D., Schlegel, H.B., DeWitt, M.J. and Drake, G.W.F., Chem. Phys. Lett., 339 (2001) 427.

[18] Shi, D.H., Sun, J.F., Zhu, Z.L. and Liu, Y.F., Chin. Phys. Soc., 16 (9) (2007) 2701.

[19] Uhlenbeck, G.E. and Beth, E., Physica, 3 (8) (1936) 729.

[20] Beth, E. and Uhlenbeck, G.E., Physica, 4 (10) (1937) 915.

[21] Bishop, R.F., Ghassib, H.B. and Strayer, M.R., J. Low Temp. Phys., 26 (1977) 669.

[22] Ghassib, H.B., Bishop, R.F. and Strayer, M.R., J. Low Temp. Phys., 23 (1976) 393.

[23] Bishop, R.F., Ghassib, H.B. and Strayer, M.R., Phys. Rev. A, 13 (1976) 1570.

[24] Ghatee, M.H. and Sanchooli, M., Fluid Phase Equilibria, 189 (2001) 63.